Biochemistry and Biophysics Reports 26 (2021) 100928

Contents lists available at ScienceDirect

Biochemistry and Biophysics Reports

journal homepage: www.elsevier.com/locate/bbrep

Deletion of Von Willebrand A Domain Containing Protein (VWA8) raises activity of mitochondrial electron transport chain complexes in hepatocytes

Moulun Luo [a], Wuqiong Ma [a], Rocio Zapata-Bustos [a], Wayne T. Willis [a,b], Lawrence J. Mandarino [a,b,*]

[a] Department of Medicine, Division of Endocrinology, USA
[b] Center for Disparities in Diabetes, Obesity, and Metabolism, The University of Arizona, Tucson, AZ, 85724, USA

ARTICLE INFO

Keywords:
VWA8
Hepatocytes
Electron transport chain
Mitochondria

ABSTRACT

VWA8 (Von Willebrand A Domain Containing Protein 8) is a AAA+ ATPase that is localized to the mitochondrial matrix and is widely expressed in highly energetic tissues. Originally found to be higher in abundance in livers of mice fed a high fat diet, deletion of the VWA8 gene in differentiated mouse AML12 hepatocytes unexpectedly produced a phenotype of higher mitochondrial and nonmitochondrial oxidative metabolism, higher ROS (reactive oxygen species) production mainly from NADPH oxidases, and increased HNF4a expression. The purposes of this study were first, to determine whether higher mitochondrial oxidative capacity in VWA8 null hepatocytes is the product of higher capacity in all aspects of the electron transport chain and oxidative phosphorylation, and second, the density of cristae in mitochondria and mitochondrial content was measured to determine if higher mitochondrial oxidative capacity is accompanied by greater cristae area and mitochondrial abundance. Electron transport chain complexes I, II, III, and IV activities all were higher in hepatocytes in which the VWA8 gene had been deleted using CRISPR/Cas9. A comparison of abundance of proteins in electron transport chain complexes I, III and ATP synthase previously determined using an unbiased proteomics approach in hepatocytes in which VWA8 had been deleted showed agreement with the activity assays. Mitochondrial cristae, the site where electron transport chain complexes are located, were quantified using electron microscopy and stereology. Cristae density, per mitochondrial area, was almost two-fold higher in the VWA8 null cells ($P < 0.01$), and mitochondrial area was two-fold higher in the VWA8 null cells ($P < 0.05$). The results of this study allow us to conclude that despite sustained, higher ROS production in VWA8 null cells, a global mitochondrial compensatory response was maintained, resulting in overall higher mitochondrial oxidative capacity.

1. Introduction

VWA8 (Von Willebrand A Domain Containing Protein 8) is a AAA+ ATPase that is localized to the mitochondrial matrix face of the inner mitochondrial membrane and is widely expressed in highly energetic tissues [1–4]. Originally this protein was found to be higher in abundance in livers of mice fed a high fat diet [3]. Deletion of the VWA8 gene in differentiated mouse AML12 hepatocytes unexpectedly produced a phenotype of higher mitochondrial and nonmitochondrial oxidative metabolism, higher ROS (reactive oxygen species) production mainly from NADPH oxidases, and increased Hepatocyte nuclear factor 4 alpha (HNF4a) expression [4]. Genes regulated by HNF4a generally had higher expression levels, suggesting that most of the phenotypic changes could be attributed to the rise in HNF4a. This may have been the result of an effort to compensate for the loss of VWA8 function [4]. The gene expression and protein abundance response produced higher levels of oxidative metabolism. This was especially true for mitochondrial fuel oxidation but also was the case for other sites of oxygen consumption, including peroxisomes and other oxidases [4].

It is likely that the sustained increases in ROS production, HNF4a

Abbreviations: ADP, adenine dinucleotide phosphate; ANT, adenine nucleotide translocase; ATP, adenine trinucleotide phosphate; ETC, electron transport chain; HNF4, hepatocyte nuclear factor 4; NADPH, nicotinamide adenine dinucleotide phosphate; OCR, oxygen consumption rate; PFO, perfringolysin; ROS, reactive oxygen species; TMHQ, Tetramethylhydroquinone; TMPD, N,N,N′,N’-Tetramethyl-p-phenylenediamine; VWA8, Von Willebrand Domain-containing Protein 8.

* Corresponding author. Division of Endocrinology, Department of Medicine, Center for Disparities in Diabetes, Obesity, and Metabolism, University of Arizona, 1501 N. Campbell Ave, Tucson, AZ, 85724, USA.
E-mail address: mandarino@deptofmed.arizona.edu (L.J. Mandarino).

https://doi.org/10.1016/j.bbrep.2021.100928
Received 19 August 2020; Received in revised form 19 January 2021; Accepted 19 January 2021

expression and mitochondrial fuel oxidation during the time course of differentiation of AML12 hepatocytes were due to the inability of this compensatory response in cells lacking VWA8 to normalize some aspects of mitochondrial function. VWA8 has homology with mitochondrial chaperone proteins and proteases and shares their structural characteristics [2]. Therefore, deletion of VWA8 may produce a sustained mitochondrial stress response, sensed by NADPH oxidases that continue to produce ROS even while the cell responds with higher HNF4a, leading to continued higher oxidative capacity [4]. Thus, it is possible that even though mitochondrial fuel oxidation is higher following deletion of VWA8, there could be sustained mitochondrial defects induced by higher ROS along with any defects due to the absence of VWA8. The present study was designed to determine if there is evidence for such defects in mitochondrial electron transport or mitochondrial morphology. The specific purposes of this study were two-fold. First, to determine whether higher mitochondrial oxidative capacity in VWA8 null hepatocytes is the product of higher capacity in all aspects of the electron transport chain and oxidative phosphorylation or if there are selective defects. Second, the density of cristae in mitochondria and mitochondrial content was measured to determine if higher mitochondrial oxidative capacity is accompanied by greater cristae area and mitochondrial abundance.

2. Methods

2.1. Cell culture and assay of electron transport chain complex activities

Culture and differentiation of wild type and VWA8 null AML12 hepatocytes was performed as described [1]. Monoclonal cell lines C-WT#6–8 and C-KO#6–10 were seeded in Seahorse V28 cell culture microplates (Seahorse Bioscience #100882-004, 24-well plates) at a density of 10,000 cells per well. Cells were differentiated with 0.2% FBS for 5 days, as described [4].

All Seahorse assays generally followed Seahorse Bioscience protocols, using an XFe 24 Extracellular Flux Analyzer (Seahorse Bioscience). The individual components in these assays are oligomycin (Sigma #O4876), FCCP (Sigma #C2920), rotenone (Sigma #R8875), antimycin A (Sigma #A8674), BSA (Sigma #A7030), glutamate (Sigma #1149), malic acid (Sigma #112577), pyruvic Acid (Sigma #S107360), ADP (Sigma #A5285), succinic acid (Sigma #S3674), malonic acid (Sigma #68714), PFO (Perfringolysin, ATCC #BTX-100), TMHQ (Tetramethylhydroquinone, TCI #T0822), ascorbic acid (Sigma #A5960), TMPD (Sigma #7394, N,N,N′,N'-Tetramethyl-p-phenylenediamine), 1 × MAS Buffer (220 mM Mannitol, 70 mM Sucrose, 10 mM KH_2PO_4, 5 mM $MgCl_2$, 2 mM HEPES, 1 mM EGTA, 0.2% fatty acid free BSA). In every condition in all Seahorse assays, the measurement period for oxygen consumption was 2 min.

Assays of electron transport chain complexes were performed using modifications of the methods of [5]. For Complex I and II activities, assay medium consisted of 1 nM PFO (plasma membrane permeabilizer) and Glu/Pyr/Mal/ADP (10 mM glutamate, 5 mM pyruvate, 2.5 mM malate, 2 mM ADP) in 1 × MAS Buffer. Injection Port A contained the Complex I inhibitor rotenone (final concentration 2.0 μM); Port B contained the Complex II substrate succinate (final concentration 10 mM); Port C contained the Complex II inhibitor malonate (final concentration 10 mM).

For Complex I and III activities, assay medium consisted of 1 nM PFO and Glu/Pyr/Mal/ADP in 1 × MAS Buffer. Injection Port A contained Complex I inhibitor rotenone (final 2.0 μM) and Complex II inhibitor malonate (final concentration 10 mM); Port B contained Complex III substrate TMHQ (final 0.4 mM); Port C contained the Complex III inhibitor antimycin A (final concentration 10 μM).

For Complex IV activity, assay medium consisted of 1 nM PFO, Complex I inhibitor rotenone (final concentration 2.0 μM), Complex III inhibitor antimycin A (final concentration 2.0 μM), Complex IV substrates TMPD/ascorbate (final concentrations 1 mM/5 mM) and ADP (final concentration 2 mM) in 1 × MAS Buffer; Injection Port A was Complex IV inhibitor sodium azide (20 mM).

2.2. Proteomics analysis

Global protein abundance was determined as described [1]. Aggregated results for protein subunits of electron transport chain complexes and other proteins that are reported here were included individually in Supplemental Table 6 of a previous publication [4].

2.3. Electron microscopy and measurement of cristae abundance using stereology

AML12 hepatocytes were cultured on Aclar film as described [6]. Fixation of cells and embedding was performed as described [6]. Transmission electron microscopy, at an accelerating voltage of 80 kV, was conducted at the Mayo Clinic Microscopy and Cell Analysis core.

An index of cristae abundance relative to mitochondria area was measured by stereology, using a modification of the techniques of Nielsen et al. and Weibel [7,8]. A 20X20 grid of 100 nm squares (each square was 5 × 5 nm) was placed on transmission electron microscopy images at a magnification of 40,000×. Mitochondria in the images were identified as organelles around which a double membrane could readily be seen. Corners of individual squares in the grid were counted when they were within a mitochondrion. Cristae were counted where they crossed any line in the grid within a mitochondrion. The ratio of cristae to mitochondria counts was used as an index of cristae density. Mitochondrial area of same-sized images was taken as total number of grid box corners counted within mitochondria. Ten images (five each from wild type and VWA8 null AML12 hepatocytes) were randomly selected and assigned codes. Two reviewers who were blind to the genotype of the cells counted cristae and mitochondria.

3. Results

3.1. Electron transport chain complex activities

The Seahorse XFe 24 metabolic analyzer was used to assay the activities of ETC complexes I-IV by monitoring rates of oxygen consumption (OCR) in permeabilized AML12 hepatocytes. The results of these assays are depicted in Fig. 1 and quantitative results are given in Table 1. With the use of specific substrates, electrons were delivered to each of the four ETC complexes in three separate Seahorse experiments, each performed independently four times. All ETC assays included 2 mM ADP to activate maximal rates of oxidative phosphorylation. In the first assay (Fig. 1A), electron entry at Complex I was achieved by adding glutamate, pyruvate, and malate. Complex I activity was inhibited by rotenone, and the difference between OCR determined in the presence and absence of rotenone was taken as Complex I activity. In this same assay it was possible to determine Complex II activity by subsequent addition of succinate followed by the addition of malonate to inhibit Complex II activity. In the second set of assays, Complex I activity was determined as above and after inhibition of Complex I activity with rotenone, TMHQ (4 nM) was added as an electron donor to Complex III. Complex III activity was then determined as the difference between this rate and that obtained after addition of Antimycin A, a Complex III inhibitor (Fig. 1B). Finally, Complex IV activity was determined using TMPD and ascorbate, an electron donor to Complex IV, in the presence of rotenone and antimycin A to inhibit Complexes I and III. Complex IV activity was the difference between this rate of oxygen consumption and that determined after inhibition of Complex IV with sodium azide (Fig. 1C).

The activities of the ETC complexes are given in Table 1. Complex I, II, III, and IV activities were approximately 1.6, 1.8, 1.6, and 1.6-fold higher in VWA8 null hepatocytes than in wild type AML12 hepatocytes. All were statistically significant, as indicated in Table 1.

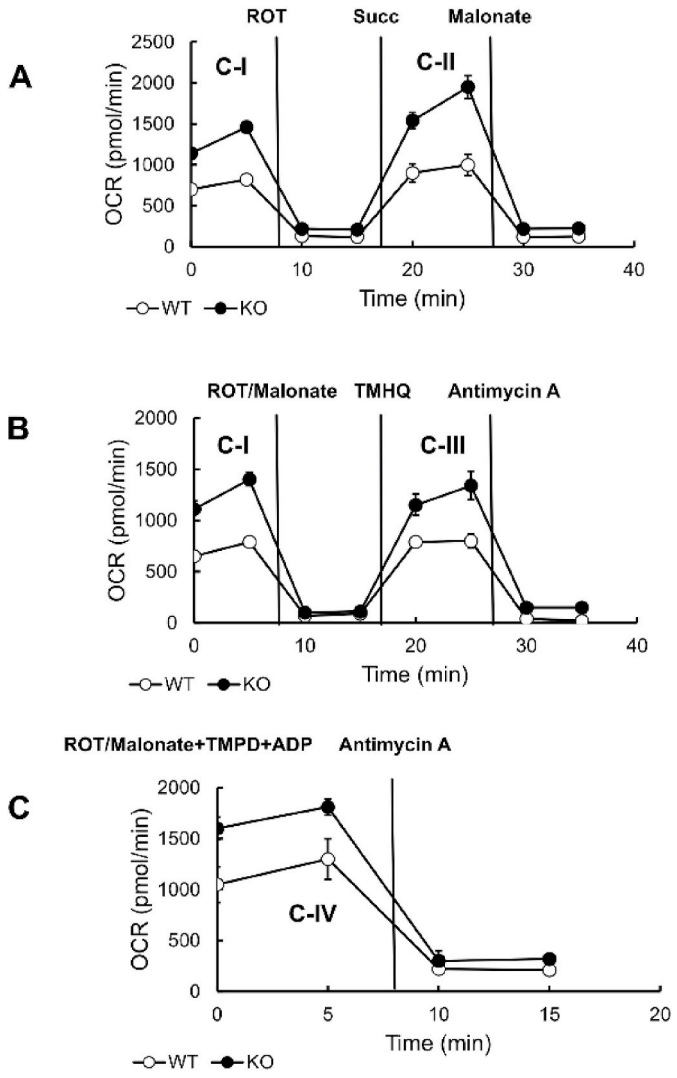

Fig. 1. Activities of ETC (electron transport chain) complex activities. Complex I and II activities are given in (A), Complex I and III activities in (b), and complex IV in (C). Activities were assayed in the Seahorse XFe 24 analyzer as described in the text. Activities from permeabilized wild type AML12 hepatocytes are shown as open circles and from VWA8 null cells as closed circles (Mean ± SD). Data are from four biological replicates each of wildtype and VWA8 null AML12 hepatocytes.

Table 1
Activities of electron transport chain complexes.

	n	Wild type	VWA8 null
Experiment set 1			
Complex I	4	666 ± 71	1151 ± 46***
Complex II	4	845 ± 62	1554 ± 57***
Experiment set 2			
Complex I	4	709 ± 29	1098 ± 107*
Complex III	4	693 ± 101	1087 ± 110**
Experiment set 3			
Complex IV	4	935 ± 55	1491 ± 75***

Activities of ETC complexes in permeabilized AML12 hepatocytes were determined as described in the Methods. Three sets of experiments were performed (n = 4 within each set, see Fig. 1). Data were calculated as described above and given as Mean ± SEM. *P < 0.05, **P < 0.01, ***P < 0.001 vs. wild type.

3.2. Proteomics analysis of electron transport chain subunits, ATP synthase, and ANT (adenine nucleotide translocase)1/2

To perform these analyses, we used protein abundance values comparing wild type and VWA8 null AML12 hepatocytes for electron transport chain complex and other proteins that were published previously and included in Supplemental Table 6 of that publication [4]. We include those values, grouped according to electron transport chain complexes I-V (ATP synthase) and adenine nucleotide translocase 1 and 2 in Supplemental Table 1. Values are given as normalized, transformed protein abundance values and further normalized to a value of 1.0 for values for each protein in the wild type cells (fold change induced by deletion of VWA8). Average values for VWA8 null cells for each protein in an ETC complex were compared with a value of 1.0 using one-sample t-tests. ETC complexes I, III, and V (ATP synthase) all had higher overall values for protein abundance in the VWA8 null cells (Fig. 2). ATP synthase was particularly high in the VWA8 null cells, with 14 of 16 subunits detected having higher values. Abundance of proteins in ETC complexes II and IV were not significantly greater in the VWA8 null hepatocytes. Likewise, neither ANT1 nor ANT2 differed in abundance between wild type and VWA8 null cells. ANT2 appeared to be the major isoform in AML12 hepatocytes, as it is in liver *in vivo* [9], being about an order of magnitude greater in abundance than ANT1. In wild type cells, the abundance of ANT2 was $4.46 \pm 0.33 \times 10^9$ normalized intensity units compared to a value of $7.58 \pm 0.58 \times 10^8$ for ANT1. This ratio was maintained in VWA8 null cells, where the abundance of ANT2 was $4.34 \pm 0.26 \times 10^9$ and that of ANT1 was $6.76 \pm 0.26 \times 10^8$.

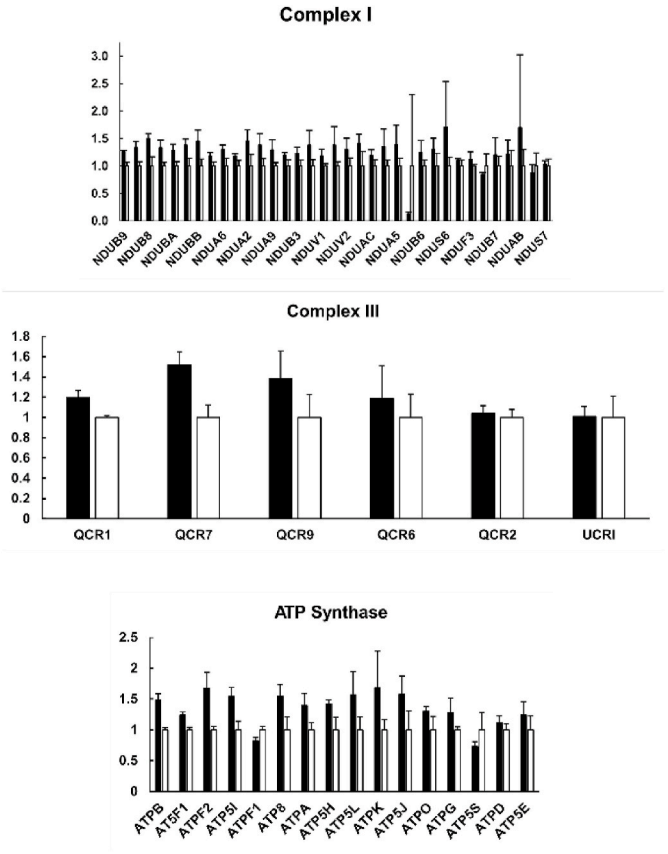

Fig. 2. Protein abundance values for electron transport complexes I, III, and ATP synthase. Values are shown as Mean ± SEM, where abundance values are normalized to an average of 1.0 for each subunit for wildtype AML12 hepatocytes. All three complexes were significantly (P < 0.05) different between wildtype (open bars) and VWA8 null (closed bars) hepatocytes. Individual values are given in Supplemental Table 1. Data are from three each biological replicates from wildtype and VWA8 null AML12 hepatocytes.

3.3. Mitochondrial cristae density and mitochondrial area

Two observers scored cristae density in a blinded fashion, using electron micrographs of wild type and VWA8 null AML12 hepatocytes. There was good agreement between the observers for the density of cristae relative to mitochondrial area (Fig. 3A), with a correlation coefficient of 0.80 ($P < 0.01$). Mitochondria accounted for a greater area in electron micrographs of VWA8 null vs. wild type AML12 hepatocytes (446 ± 93 vs. 207 ± 98 counts, $P = 0.012$).

4. Discussion

In a previous study [4], we showed that deletion of VWA8 in AML12 hepatocytes raised the overall level of cellular oxidation of lipid and carbohydrate fuels. In intact cells, the rate of fuel oxidation is controlled not only at sites of oxidation, such as mitochondria, peroxisomes, or other oxidases such as cytochrome P450 enzymes, but also by fuel delivery systems such as plasma membrane fuel transporters, intracellular lipid binding, transporting and activating proteins, and the glycolytic pathway. However, permeabilized cells allow a more direct examination of mitochondrial function because equilibration of the cytosol with extracellular medium allows direct access of metabolites and other substances to mitochondria [10]. In permeabilized cells it is possible to provide both oxidative substrates and ADP at known, saturating levels to assess "maximal" rates of mitochondrial oxidative phosphorylation. Our analysis of permeabilized AML12 hepatocytes showed that VWA8 null hepatocytes had dramatically higher mitochondrial oxidative capacity. The differences previously observed in intact cells could be explained in part by changes in expression of proteins involved in fuel delivery [4]. Additionally, we provided evidence that when differences in fuel delivery through the plasma membrane or cytosol were removed by studying cells in which the plasma membrane had been permeabilized, rates of oxygen consumption in response to carbohydrate fuels were raised to an even greater extent in the VWA8 null cells [4].

In the present study, we used permeabilized wild type and VWA8 null AML12 hepatocytes to further dissect the rise in mitochondrial oxidative capacity by using various inhibitors and electron donors to assay the activities of ETC complexes I-IV [5]. We previously showed the

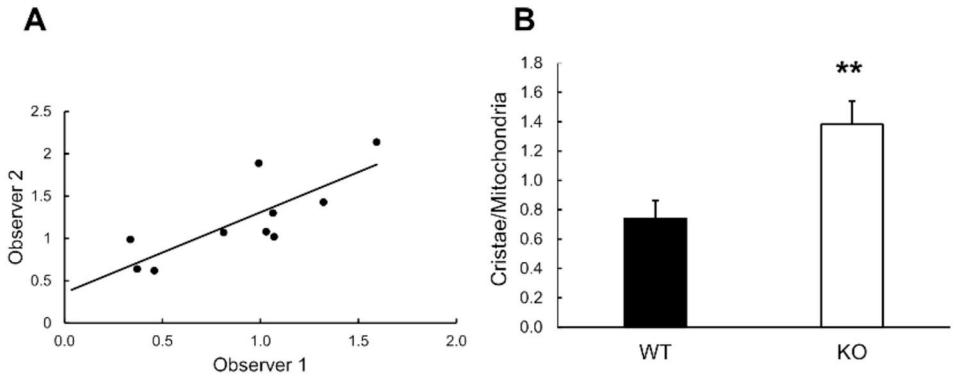

Fig. 3. Mitochondrial cristae density and area. Cristae and mitochondria were counted as described in the Results. (A) Correlation of values for cristae/mitochondria in two independent, blinded observers; (B) Cristae/mitochondria ratio in wildtype (WT, closed bar) and VWA8 knockout (KO, open bars). Data are Means ± SEM; Representative electron micrographs for VWA8 knockout (C) and wildtype (D) AML12 hepatocytes. Each observer counted cristae in 5 each technical replicates for wildtype and VWA8 null AML12 hepatocytes. Replicates were separate AML12 cells chosen because the entire cell could be visualized clearly.

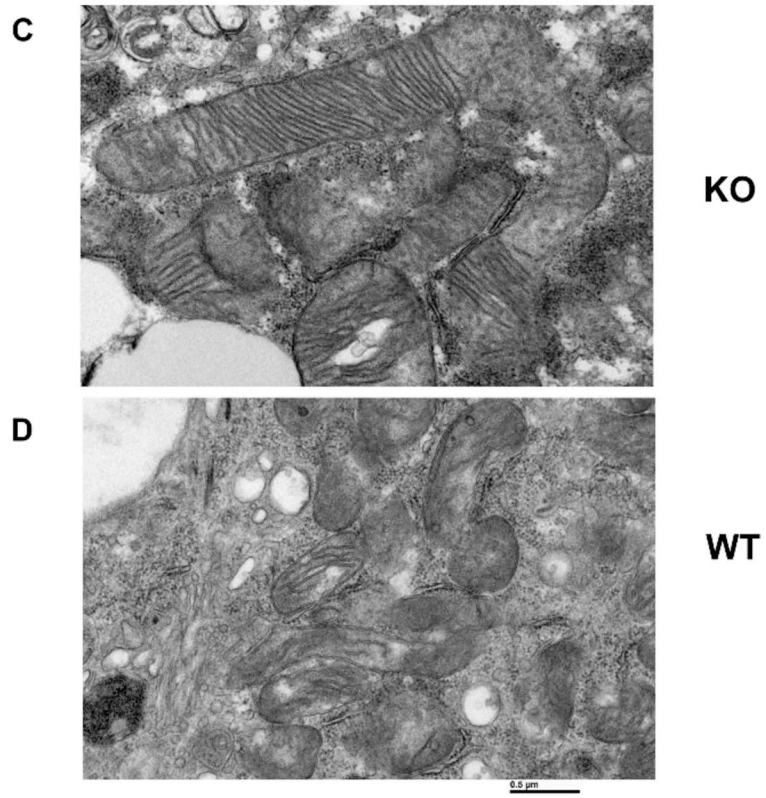

overall rate of oxidative phosphorylation was higher in VWA8 null hepatocytes [4]. The results of the current study definitively show that all the components of the electron transport system are proportionally higher upon deletion of VWA8. Therefore, there is no evidence that there are selective changes in oxidative phosphorylation produced in response to deletion of this mitochondrial protein. However, it must be noted that when activities of electron transport chain activities are assayed using the rate of oxygen consumption, these activities are dependent upon the flow of electrons from the complex being measured to Complex IV and the activity of Complex IV itself. Therefore, the measures of activity presented here, except for Complex IV itself, are not pure measures of isolated ETC complex activity. Complex IV activity, when studied in isolation, was higher in the VWA8 null hepatocytes. It is not possible from these activity assays to conclude decisively that the activities of Complexes I and III, for example would be higher absent the higher Complex IV activity. However, these two complexes also had higher levels of protein abundance in the VWA8 null hepatocytes, providing independent evidence that their activities likely were increased by deletion of VWA8 and the response of HNF4a. Another limitation of this method is that because of limited solubility of some electron donors such as TMHQ, maximal concentrations of such donors are difficult to achieve. This may have been evidenced by higher OCR using succinate than TMHQ. Moreover, Complex V, or ATP synthase had higher levels of protein abundance, consistent with higher oxidative phosphorylation in the VWA8 null hepatocytes [4]. When oxygen consumption stimulated by saturating ADP is used as a measure of complex activity, the activity of Complex V also is involved. Higher rates of oxygen consumption in response to carbohydrate fuels also suggest higher activities of substrate dehydrogenases in the knockout cells [4]. Nevertheless, the comparison of wild type and VWA8 null cells should be generally valid since both were studied using the same conditions. It should be noted that the use of artificial electron donors such as TMHQ and TMPD is non-physiologic. However, our goal was to estimate, in one common environment, the relative activities of ETC complexes in wildtype and VWA8 null AML12 cells. So although the assays may not be physiological, differences due to deletion of VWA8 should at least be directionally accurate.

The following model was previously proposed as a mechanism to explain the sustained compensatory response in oxidative metabolism in hepatocytes lacking VWA8 [4]. Because VWA8 has structural characteristics of a mitochondrial chaperone [4], it can be hypothesized that the rise in oxidative capacity when VWA8 is deleted is due to an effort to compensate for the loss of VWA8. This could raise ROS production from NADPH oxidases, primarily NOX4, which sense mitochondrial stress. The rise in ROS also produces an increase in HNF4a expression, which coordinates a gene transcription response that increases mitochondrial biogenesis, mitochondrial content and other "hepatocyte-like" features of these cells [4]. However, the compensatory response does not repair the loss of VWA8, so this defect sustains the stress response [4].

We analyzed our previously reported proteome data [4] to determine if the higher ETC complex activities observed in this study could be explained by higher abundance of their protein subunits. Protein abundance for complex I and III subunits were significantly higher in VWA8 null cells, as were many subunits of ATP synthase, consistent with the results of the ETC complex activity assays. Proteins involved in complexes II and IV, however, were not significantly higher in the VWA8 null cells. One assembly factor for complex II, SDHf3 was higher in the knockout cells [4] and possibly could explain higher complex II activity. Regarding complex IV, the difference between the activity assays and proteomic results cannot be experimentally explained by this study. However, post-translational modifications that affect activity, although not assessed here, could be affecting activities or assembly of proteins. Additionally, higher Complex V activity, as evidenced by higher ADP-stimulated oxygen consumption in the VWA8 null cells, also might be implicated in this phenomenon. Finally, as may have been the case for Complex II, higher efficiency or overall rates of assembly of electron transport chain complexes may also be involved.

Results from stereological measurement of cristae density showed that cristae were more numerous in mitochondria from VWA8 null AML12 hepatocytes. In addition, although not strictly a measure of mitochondrial volume density, cross-sectional area of mitochondria also was higher in VWA8 null cells. These results indicate, then, that deletion of VWA8 results in an overall rise in mitochondrial abundance, electron transport chain activity, and oxidative phosphorylation. When taken together with previous results, the current findings suggest that a higher HNF4a response to stress resulting from deletion of VWA8 leads to a generalized overcompensation in mitochondrial oxidative metabolism. There is no evidence of selective defects in the electron transport chain or mitochondrial morphology related to a sustained, higher level of reactive oxygen species.

Author statement

Moulun Luo: Conceptualization, Methodology, Investigation, Formal analysis, Writing Original Draft

Wuqiong Ma: Methodology, Investigation

Rocio Zapata-Bustos: Methodology, Investigation

Wayne T. Willis: Conceptualization, Methodology, Investigation, Formal analysis, Writing Original Draft

Lawrence J. Mandarino: Conceptualization, Methodology, Validation, Investigation, Formal analysis, Resources, Data Curation, Writing Original Draft, Writing Review and Editing, Visualization, Supervision, Project administration, Funding acquisition.

Disclosure statement

The authors have nothing to disclose.

Declaration of competing interest

The authors declare that they have no known competing financial interests or personal relationships that could have appeared to influence the work reported in this paper.

Acknowledgements

This work was supported in part by NIH grant R01DK067496 (LJM). Scott Gamb of the Mayo Clinic Microscopy and Cell Analysis Core Facility performed the electron microscopy.

Appendix A. Supplementary data

Supplementary data related to this article can be found at https://doi.org/10.1016/j.bbrep.2021.100928.

References

[1] M. Luo, W. Ma, Z. Sand, J. Finlayson, T. Wang, R.D. Brinton, W.T. Willis, L. J. Mandarino, Von Willebrand factor A domain-containing protein 8 (VWA8) localizes to the matrix side of the inner mitochondrial membrane, Biochem. Biophys. Res. Commun. 521 (2020) 158–163.

[2] M. Luo, A.E. Mengos, W. Ma, J. Finlayson, R.Z. Bustos, Y. Xiao Zhu, C.X. Shi, T. M. Stubblefield, W.T. Willis, L.J. Mandarino, Characterization of the novel protein KIAA0564 (Von Willebrand domain-containing protein 8), Biochem. Biophys. Res. Commun. 487 (2017) 545–551.

[3] M. Luo, A.E. Mengos, T.M. Stubblefield, L.J. Mandarino, High fat diet-induced changes in hepatic protein abundance in mice, J. Proteonomics Bioinf. 5 (2012) 60–66.

[4] M. Luo, W.T. Willis, D.K. Coletta, P.R. Langlais, A. Mengos, W. Ma, J. Finlayson, G. R. Wagner, C.X. Shi, L.J. Mandarino, Deletion of the mitochondrial protein VWA8 induces oxidative stress and an HNF4alpha compensatory response in hepatocytes, Biochemistry 58 (2019) 4983–4996.

[5] J.K. Salabei, A.A. Gibb, B.G. Hill, Comprehensive measurement of respiratory activity in permeabilized cells using extracellular flux analysis, Nat. Protoc. 9 (2014) 421–438.

[6] R.E. Kingsley, N.L. Cole, Preparation of cultured mammalian cells for transmission and scanning electron microscopy using Aclar film, J. Electron. Microsc. Tech. 10 (1988) 77–85.

[7] J. Nielsen, K.D. Gejl, M. Hey-Mogensen, H.C. Holmberg, C. Suetta, P. Krustrup, C.P. H. Elemans, N. Ortenblad, Plasticity in mitochondrial cristae density allows metabolic capacity modulation in human skeletal muscle, J. Physiol. 595 (2017) 2839–2847.
[8] E.R. Weibel, in: Theoretical Foundations, Stereological Methods. Volume 2: Theoretical Foundations, Stereological Methods, 2, Academic Press, London, 1980.
[9] A. Dorner, M. Olesch, S. Giessen, M. Pauschinger, H.P. Schultheiss, Transcription of the adenine nucleotide translocase isoforms in various types of tissues in the rat, Biochim. Biophys. Acta 1417 (1999) 16–24.
[10] S.A. Mookerjee, A.A. Gerencser, D.G. Nicholls, M.D. Brand, Quantifying intracellular rates of glycolytic and oxidative ATP production and consumption using extracellular flux measurements, J. Biol. Chem. 292 (2017) 7189–7207.